

THE BETA SPECTRUM STUDY OF  
RADIOACTIVE PHOSPHORUS

by

RANDALL EDWARD MURPHY

B. S., Washburn Municipal University, 1956

---

A THESIS

submitted in partial fulfillment of the

requirements for the degree

MASTER OF SCIENCE

Department of Physics

KANSAS STATE UNIVERSITY  
OF AGRICULTURE AND APPLIED SCIENCE

1959

LD  
2668  
T4  
1959  
M87  
C.2  
Documents

TABLE OF CONTENTS

|                                                          |    |
|----------------------------------------------------------|----|
| INTRODUCTION AND REVIEW OF LITERATURE . . . . .          | 1  |
| THEORY OF BETA DECAY . . . . .                           | 2  |
| SMALL ORDER EFFECTS IN PHOSPHORUS 32 . . . . .           | 9  |
| APPARATUS . . . . .                                      | 10 |
| EXPERIMENTAL TECHNIQUES AND PROCESSING OF DATA . . . . . | 14 |
| RESULTS AND CONCLUSIONS . . . . .                        | 30 |
| ACKNOWLEDGMENT . . . . .                                 | 32 |
| LITERATURE CITED . . . . .                               | 33 |

## INTRODUCTION AND REVIEW OF LITERATURE

At the turn of the century it was found that certain naturally occurring substances such as Ra E emitted particles which had the same  $e/m$  ratio as electrons. The charge to mass ratio helped to establish that the emitted particles, called beta rays, were electrons. Neither the rate of decay nor the number of electrons given off from a sample could be altered by any physical or chemical means yet electrons appeared spontaneously. The spontaneous emission indicated that the electrons were of nuclear origin. Since the nucleus had discrete energy levels, the energy of an electron could come from an excited nucleus in its attempt to become energetically stable. If such were the case, it would be expected that the energy of every electron of a particular substance would be the same and characteristic of the transition. Absorption data and energy determinations by magnetic deflection techniques showed that beta rays had a continuous energy distribution. A continuous energy spectrum for beta rays appeared to be a serious contradiction to the law of conservation of energy.

Pauli proposed that in addition to an electron, a second particle, called the neutrino, was emitted simultaneously in such a way as to conserve energy. The neutrino had to have unusual properties to account for its being unobserved in the beta spectrum. Specifically, the neutrino had to be electrically neutral, have a rest mass very nearly zero, and have a spin of  $\frac{1}{2}$ . The spin of  $\frac{1}{2}$  was necessary in order for angular momentum to be conserved.

In 1934 Fermi (5) gave the first successful theory of beta decay making use of the Pauli neutrino. The correctness of the theory proposed by Fermi was not borne out by early experiments. The discrepancies between the experimental evidence and theory were due primarily to poor experimental

techniques such as source thickness and back scattering. More recently, however, investigations of the large number of artificially produced beta emitters have presented overwhelming evidence in favor of the Fermi theory and have made its acceptance universal.

Artificially produced beta emitting isotopes have been obtained with high specific activity, thereby enabling the beta spectrum to be investigated for small order effects. The absence or presence of small order effects caused by interference was shown by Fierz (6), as a supplement to the Fermi theory, to be a direct indication of the type of transition that occurred in a decaying nucleus. The exact transition that is effected in beta disintegration has remained of basic importance, and its understanding would represent a tremendous advancement in nuclear physics. The salient features of the theory of beta decay will be presented here to provide background for the present investigation.

#### THEORY OF BETA DECAY

The basic transformations of beta decay which give a continuous energy distribution were incorporated by Fermi in a manner analogous to the emission of electromagnetic radiation in the formulation of the theory of beta decay.

$$n \longrightarrow p + e + \nu \quad (\text{neutron yields proton, electron and neutrino}) \quad (1)$$

$$p \longrightarrow e^+ + n + \nu \quad (\text{proton yields positive electron, neutron and neutrino}) \quad (2)$$

$$p + e \longrightarrow n + \nu \quad (\text{proton and electron yields neutron and neutrino}) \quad (3)$$

The emission of electromagnetic radiation described by Dirac was presented by employing quantum field theory. Field theory was utilized in order to account for the creation of photons. One consequent of the Dirac theory of singular importance was that the coupling energy per unit volume could be

represented by the following equation:

$$H = \mathbf{j} \cdot \boldsymbol{\rho} + A\bar{\phi} \quad (4)$$

where  $\mathbf{j}$  is the current density,  $\rho$  is the charge density,  $A$  and  $\bar{\phi}$  are the components of the four-vector electromagnetic potential and  $c$  is the velocity of light. Thus the coupling energy was given as the scalar product of two four-vectors.

If the nucleus is thought of as the source of the field and the electrons and neutrinos acting collectively as the field particles then the similarity between electromagnetic radiation and beta decay becomes more apparent. The similarity of these two types of reactions tends to justify the extension of Equation (4) to beta decay. Obviously the terms of Equation (4) have to be replaced by their corresponding counterparts for a nuclear transition if beta decay is to be represented. Specifically,  $\mathbf{j}$  and  $\rho$  must be replaced by the transition current and charge density in terms of the initial and final nuclear wave functions (16). Likewise,  $A$  and  $\bar{\phi}$  must be replaced by four-vector current in electron and neutrino wave functions.

Although the coupling energy for beta decay may be represented by making the appropriate substitutions, its evaluation has remained as yet unsolved. The basic obstacle encountered in attempting to evaluate the coupling energy lies in the fact that the nuclear wave functions are not known. At this point, one might be tempted to believe that a suitable theory of beta decay could be forthcoming only after the nuclear wave functions became known. Quite the contrary is true. While the exact form of interaction is not available it is expected that the forms which are present in electromagnetic radiation will also be present in the beta transition.

The exact form of transition that takes place in electromagnetic radiation is well known, further it is known that only vector and tensor

types of interactions are possible. Therefore vector and tensor forms must be investigated to establish whether or not additional forms are acceptable for beta decay. The requirement of relativistic invariance produces three distinct possibilities which transform as either a tensor or vector, namely, scalar, axial vector and pseudoscalar (2). In general the coupling energy is represented as a linear sum of the five possible forms,

$$H = G_1 H_V + G_2 H_T + G_3 H_S + G_4 H_A + G_5 H_P \quad (5)$$

where the  $G$ 's are the Fermi coupling constants and are a measure of the magnitude of each particular type of interaction. Inherent in each of the Fermi coupling constants is a universal constant ( $g$ ) analogous to the charge on the electron. While the interaction or coupling energy is presented as a linear sum it is not intended that a nonlinear combination should be excluded. The importance of the form of interaction energy can not be over-emphasized since it is the quantity foremost in producing the beta transition.

Quantum mechanically the formula first derived by Dirac (13) for the probability of transition per unit time, using time dependent perturbation theory, is

$$P(dp) = 2\pi/\hbar \left| \int \psi_f^* H \psi_i \right|^2 dN/dE_0 \quad (6)$$

In Equation (6),  $H$  is the operator associated with the interaction energy,  $\psi_i$  and  $\psi_f$  are the time dependent wave functions for the initial and final states of the system, and  $dN/dE_0$  is the energy density of the final states in real space. The quantity between bars,  $|\int \psi_f^* H \psi_i|$ , is called the matrix element of transition. Essentially then, the problem in beta decay is to evaluate the terms for the probability of transition in the simplest possible form.

The quantity  $dN/dE_0$  of Equation (6), the energy density of the final states, is evaluated by the following relations:



$$p = (E[E + 2m_0c^2])^{1/2} \quad q = 1/c (E_0 - E) \quad (7)$$

The symbols  $p$  and  $q$  are used to denote the electron and neutrino momentum respectively,  $m_0$  the rest mass of the electron,  $E_0$  the maximum beta ray energy and  $E$  the energy of the emitted electron. Strictly speaking, the neutrino momentum which is given through the energy conservation principle is not correct since the energy of the recoiling nucleus must also be included. However, the use of the neutrino momentum as given above is valid because the mass of the residual nucleus is very large and consequently its kinetic energy must be small.

Obviously, the energy density of the final states depends upon the number of states available to the electron and neutrino. It is easily shown that the number of electron states in volume  $\mathcal{V}$  with momentum between  $p$  and  $p + dp$  is  $\frac{4\pi p^2 dp \mathcal{V}}{\hbar^3}$  and similarly that the number of neutrino states between  $q$  and  $q + dq$  is  $\frac{4\pi q^2 dq \mathcal{V}}{\hbar^3}$  (10). The probability that an electron and neutrino will occupy any particular state is given by the product of the total number of states available to the leptons, thus:

$$dN/dE_0 = \frac{16\pi^2 \mathcal{V}^2 p^2 q^2 dp dq}{\hbar^6} \quad (8)$$

Equation (8) involves the neutrino momentum and it is desirable to represent the energy density of the final states as a function of the electron momentum and energy alone. Through the use of Equation (7) it is possible to change from electron-neutrino momentum space to electron momentum-energy space, that is,

$$(dp)(dq) = J(dp)(dE_0) = 1/c (dp)(dE_0) \quad (9)$$

where  $J$  is the jacobian. With this change it is possible to write Equation (8) in the following form:

$$dN/dE_0 = \frac{16\pi^2 \mathcal{V}^2 p^2 (E_0 - E)^2 dp}{\hbar^6 c^3} \quad (10)$$

The transition matrix of Equation (6) is simplified by assuming that

the wave functions for the electron and neutrino can be represented by the plane waves,

$$\Psi_p = N_p e^{i p \cdot r / \hbar} \quad \Psi_q = N_q e^{i q \cdot r / \hbar} \quad (11)$$

where  $p$  and  $q$  again represent the momentum of the electron and neutrino respectively, and  $N_p$  and  $N_q$  are the respective normalizing factors.

Normalising the wave functions over volume  $\tau$  it is found that both normalising factors have the same value, explicitly  $\sqrt{\frac{1}{\tau}}$ . In addition it is further assumed that the transition does not depend in any way upon the coupling energy so that the probability of emission depends only upon the expectation values of the electron and neutrino at the surface of the nucleus. Thus the contribution of the electron and neutrino to transition is simply:

$$|\Psi_p(r)|^2 |\Psi_q(r)|^2 \quad (12)$$

Since the diameter of the nucleus is known to be about  $10^{-12}$  cm and the wave length of the electron about  $10^{-11}$  cm it is possible to say that Equation (12) can be further reduced by letting  $r$  equal zero, that is

$$|\Psi_p(0)|^2 |\Psi_q(0)|^2 = \frac{1}{\tau^2} \quad (13)$$

The assumptions of the preceding paragraph are obvious oversimplifications partially due to the presence of the coulombic field of the nucleus and a perturbation correction is necessary. This correction is the complicated Fermi function (16) and is dependent only upon the electron momentum and the product nucleus. The effect of the Fermi function is to warp the symmetric statistical shape in such a fashion that the probability is increased for electrons in the low energy range.

When the Fermi function is denoted as  $F(Z, p)$  and the results of Equations (10) and (13) substituted into Equation (6), the transition probability becomes:

$$P(d\rho) = \frac{g^2 M^4 |P|^2 F(Z, p)}{2\pi^3 \hbar^7 c^3} [E_0 - E]^2 d\rho \quad (14)$$



By virtue of these substitutions the matrix element of Equation (6) is reduced to  $|M|$ , the transition matrix, which involves only the initial and final wave functions of the nucleus. Physically  $|M|$  is the overlap of the initial and final nuclear wave functions or more specifically the operator which changes a neutron to a proton. The above expression for the probability of transition, given by Fermi, is of particular interest since prior to 1934 all attempts to produce an analytical expression for beta decay by empirical curve fitting had proved unsuccessful. If a plot of the square root of the transition probability, or the experimentally observed disintegrations per unit time, over the product of the square of the electron momentum and the Fermi function versus electron energy is made, a straight line results. The intersection of such a line with the energy axis readily determines the maximum beta ray energy.

In optical spectra the transition matrix of Equation (5) is quite complicated so that the integral of the optical retardation factor is expanded in dipole, quadrupole, and octopole terms rather than evaluating the matrix elements. For such an expansion to be valid it is necessary that the wave length of the emitted radiation be very small in comparison to the 'diameter' of the atom. The classifications of forbiddenness in optical spectra are developed by considering the first non-zero term in the expansion. If the dipole term is zero the radiation is called first forbidden; if in addition the quadrupole term is zero then the radiation is second forbidden and so forth.

The same principles are applied to beta decay except that here the transition matrix is not known, but it is known that five forms of interaction energy are possible. The proper determination of selection rules for beta decay have to come from examining the relativistic matrix elements. However,

this is quite involved. The same results can be obtained by examining the wave function of a free electron having angular momentum as well as linear momentum.

The wave function for a free electron for small distances from the origin of the nucleus is known to be proportional to the distance from the origin raised to the orbital angular momentum power, that is  $\psi \sim r^l$  (2). For allowed transitions the angular momentum must be zero if the extension value of the nucleus is assumed to be zero. In allowed transitions the electrons and neutrinos are emitted with zero angular momentum, but it is possible for the intrinsic spins of the leptons to be aligned either anti-parallel or parallel. For the case in which the spins are anti-parallel the spin change  $\Delta J$  of the nucleus must be zero. Further, since electrons and neutrinos are fermions there is no change in parity. These two conditions known as the Fermi selection rules are written as follows:

Fermi selection rules:  $\Delta J = 0$ , no parity change

When the leptons have their spins oriented parallel, corresponding to a triplet state, again no angular momentum is involved and the spin change of the nucleus is  $\Delta J = 0, \pm 1$  ( $0 \rightarrow 0$  excluded) where there is no parity change.

The conditions for the triplet state are called the Gamow-Teller selection rules and are written:

Gamow-Teller selection rules:  $\Delta J = 0, \pm 1$  ( $0 \rightarrow 0$  excluded), no parity change

In the relativistic treatment of the transition matrix elements it is found that the scalar and vector interactions give rise to the Fermi selection rules whereas the Gamow-Teller selection rules are obeyed by tensor or axial vector interactions. The pseudoscalar interaction involves a parity change and therefore is not expected unless in combination with one of the other possible forms. From this it is understandable that the  $|M|$  of

Equation (4) should be replaced by the following expression:

$$M = [(V^2 + S^2)|M|^2] + [(A^2 + T^2)|M|^2] \quad (15)$$

The abundance of forbidden transitions shows that in some cases the zero extension of the nucleus is a poor approximation and that the wave length to nuclear 'diameter' ratio is not sufficiently large to justify an approximation of this nature. The degree of forbiddenness is often estimated from "ft" values. The probability of transition is the familiar decay constant and its reciprocal the mean life. Thus, if the reciprocal of the probability function is integrated over all possible values of the electron momentum, an analytic expression for the mean life is obtained. The integral of the Fermi function can be evaluated analytically only when the nuclear charge is zero, however, appropriate values for specific isotopes are obtained from graphical integration. The mean life for a specific isotope is dependent only on the integral of the transition matrix and evidently a measure of forbiddenness.

#### SMALL ORDER EFFECTS IN PHOSPHORUS 32

The beta radiations of  $P^{32}$  have been extensively investigated (1), (7), (14), (19), but only recently has emphasis been placed upon small order effects. The exact form of the law of beta decay has not been determined, since the Fermi theory contains five possible interactions. From the accumulated data involving beta decay certain combinations of the five forms are most probable, but the ultimate answer must come from angular correlation experiments. Mahmoud and Konopinski (9) proposed an STP type of combination over a VTP combination. The feasibility of such a proposal may be obtained by examining  $P^{32}$  for a Fierz type interference (6).

A Fierz interference is manifest in a reciprocal energy term multiplying

the statistical factor and is an indication of the tensor-axial vector admixture for Gamow-Teller transitions. If a Fierz interference is present then the Fermi plot would no longer be linear and its deviation would be a measure of the admixture contribution.  $P^{32}$ , with high disintegration energy and low atomic number, would tend to maximize the presence of Fierz interference. Until 1957 the linearity of the Fermi plot was not seriously questioned (4), (12) but Porter et al., (11) have obtained a shape factor plot with a significant slope. An STP combination would be quite unacceptable if such a deviation persisted.

#### APPARATUS

The 180 degree variable field magnetic focusing spectrometer-spectrograph employed in this investigation is shown in Plate I. This instrument has been described in detail elsewhere (8). The current for the energizing coils of the spectrometer was supplied by 100-ampere hour lead storage cells, and fields of constant value were maintained for periods of four hours without adjustment. Field measurements were made by balancing, through a potentiometer arrangement, the emf's of the two identical coils, one rotated in the spectrometer field and the other in a standard permanent magnet. Operating pressures of one micron were accomplished with a Cenco forepump connected in series with a one stage diffusion pump.

The spectrometer insert (Plate II, Fig. 1) has rounded baffles which have been coated with lamp black to prevent localized charge accumulation. Direct gamma rays from the source to the counting tube are absorbed by a large lead block surrounded by lucite.

End window Geiger tubes (3) were constructed to provide a means of detection and are shown in Plate II, Fig. 2. Each tube casing was of 1/8 inch

wall brass tubing, 1 inch outside diameter,  $5 \frac{1}{4}$  inches long, and provided with a  $\frac{3}{8}$  inch flange at one end to facilitate sealing the window. A second flange  $\frac{1}{4}$  inches from the end window was attached to allow the tube to be connected to the face plate of the spectrometer. A 3.1 mil diameter, 1 inch long nichrome wire was spotwelded to a 50 mil tungsten wire sealed in a glass cap. The spotweld and the end of the nichrome wire were tipped with soft glass to form a  $\frac{1}{16}$  inch diameter bead. The cap and wire assembly were sealed in the casing with a thermoplastic resin (8). The lengths of the wires were such that the tipped nichrome wire was as close to the window as possible and yet not in contact. Mica of approximately 1 milligram per square centimeter was used as window material. The uniformity of the mica was determined by examination between crossed polaroids.

The mica was sealed to the  $\frac{3}{8}$  inch flange with an ether resin (20) that possesses unique properties which make it ideal for this purpose. A washer of the same dimensions as the end window flange was sealed over the window for additional support. A filling system independent of the spectrometer was constructed which consisted of a mercury manometer, ethyl alcohol and argon bottles and a thermocouple pressure indicator. The alcohol was made water free by placing magnesium in commercially pure ethyl alcohol and distilling. The Geiger tubes were evacuated and argon and ethyl alcohol were admitted in a ratio of three to one to a pressure of about four and one-half centimeters of mercury. Several tubes were produced with plateaus of 250 volts and less than 5 percent rise per 100 volts. A typical curve is shown in Plate II, Fig. 3.

Calibration was accomplished by extrapolating the high energy edge of the 661.65 KEV internal conversion 'K' line of  $\text{Cs}^{137}$  (16). This calibration together with the determination of the resolution (Plate III) was in complete

EXPLANATION OF PLATE I

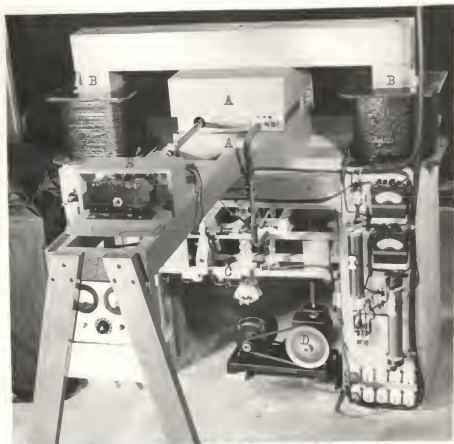
Spectrometer and auxiliary equipment

- A - Soft iron pole pieces
- B - Energising coils
- C - Diffusion pump
- D - Forepump
- E - Standard field magnet

From previous calibration and the linearity of the helipot in the potentiometer arrangement it was possible to measure fields to within one-hundredth of a gauss. For fields of 200 gauss measurements reproducible to two parts in ten thousand have consistently been obtained.



PLATE I



agreement with the original calibration of the instrument in 1953.

#### EXPERIMENTAL TECHNIQUES AND PROCESSING OF DATA

Carrier-free radioactive  $P^{32}$  was obtained from the Oak Ridge National Laboratories and was employed exclusively in this investigation. The phosphorus was produced by a neutron to proton transition of  $S^{32}$  and reportedly was greater than 99 percent pure. The chemical form of the  $P^{32}$  was  $H_3PO_4$  in a 0.5 normal solution of hydrochloric acid.

A 1 millimeter by 4 centimeter strip of aluminum foil, of thickness 0.00025 inch, was used as a backing for the source. A thickness of this order reduced back scattering and absorption to a negligible extent. Insulin was spread over the surface of the aluminum to serve a dual purpose, first to facilitate uniform spreading of the radioactive material and second to act as a buffer between the acidic source and the aluminum backing. The radioactive materials were confined to the center section of the strip of length equal to the inside diameter of the Geiger tube. This source length was used in order to minimize counts due to electrons whose trajectories were excessively oblique.

Without utilizing vacuum evaporation techniques it was impossible to place more than 5 microliters of the source material on the strip without flaking off the insulin. Pure aluminum, aluminum treated with phosphorous acid, and albumin were used in an attempt to find a 'sticking agent' which would allow a greater amount of phosphorus to be placed on the backing. Insulin was found to be more satisfactory than any of the above mentioned treatments even though it limited the amount of material that could be placed on the strip. Since only 5 microliters were placed on the backing the counting rate obtained was relatively low, that is just two or three times above

EXPLANATION OF PLATE II

Fig. 1. Spectrometer insert

Fig. 2. Geiger tube

Fig. 3. Typical Geiger tube plateau

## PLATE II

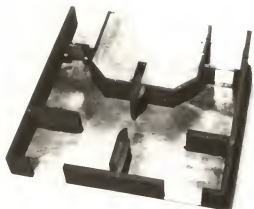


Fig. 1

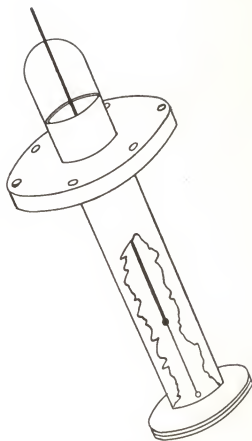


Fig. 2

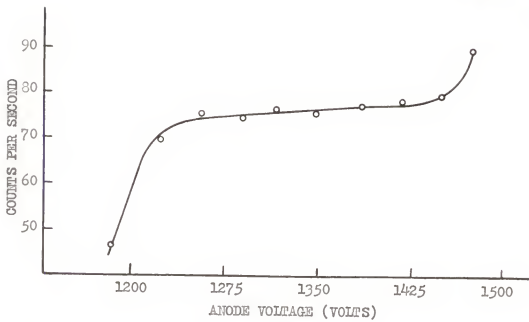


Fig. 3

### EXPLANATION OF PLATE III

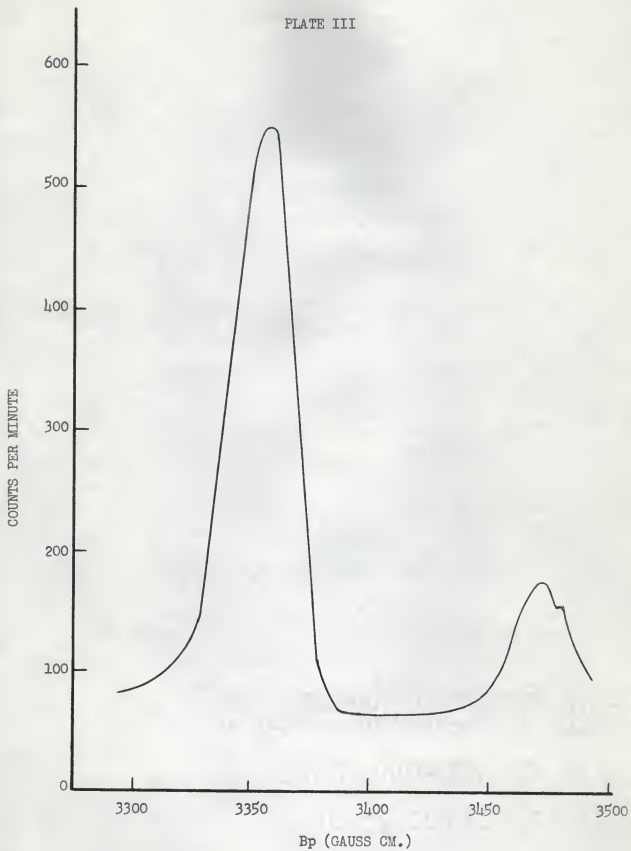
#### Internal conversion spectrum of Cs<sup>137</sup>

The intensity and position of the 'K' conversion line of Cs<sup>137</sup> with respect to the beta spectrum made it well suited for calibration purposes. The resolution of a spectrometer is the extent to which it is possible to distinguish between conversion lines with small energy separation. The resolution may be determined from the following relation:

$$R = \frac{\Delta(Bp)}{Bp}$$

where  $\Delta(Bp)$  is the half width of the conversion line and  $Bp$  the magnetic rigidity at which the line occurs. In a variable field spectrometer the trajectory of the electrons is fixed and therefore the resolution is constant independent of the particular energy used for evaluation. With the source and acceptance slit set at 1 millimeter the resolution was less than 1 percent. No attempt was made to resolve the 'L' and 'M' lines.

PLATE III





the background level at the high energy end of the spectrum.

The spectrometer was operated with 1 percent resolution over a period of twenty days. During the first few days the entire spectrum was surveyed twice to establish the general shape and also to ascertain that no unusual discrepancies were present. Counting rates for particular field settings were then established over longer periods of time to obtain the statistics necessary for a small order investigation.

The background counting rate was measured in the spectrometer by reversing the magnetic field causing the emitted electrons of the source to be bent away from the counting tube. The background level was measured both before and after data was taken of phosphorus and the average of the two background readings was used as the best estimate of background over the counting period. Since the background counting rate was comparable to the counting rate of the phosphorus the accumulated data was naturally corrected for the background contribution. Also, half-life corrections were made by correcting counting times to twelve noon of the first day of counting. The half-life of  $P^{32}$  was experimentally determined and an explanation of the results obtained can be found on page 22. With counting rates as low as were encountered, errors due to counter dead time and electronic delays were quite unimportant.

The uncertainty associated with the corrected counting rate was obtained by taking the square root of the sum of the squares of the uncertainties in the background and in the phosphorus counting rates. The uncertainty attributed to background was taken from the lump sum of all the counting times. Handling the data in this manner showed that the contribution of background was very slight in comparison to that of the phosphorus.

The normalized spectrum obtained is shown in Plate IV. This spectrum exhibited two unusual and unexpected traits. First, there appeared a definite

## EXPLANATION OF PLATE IV

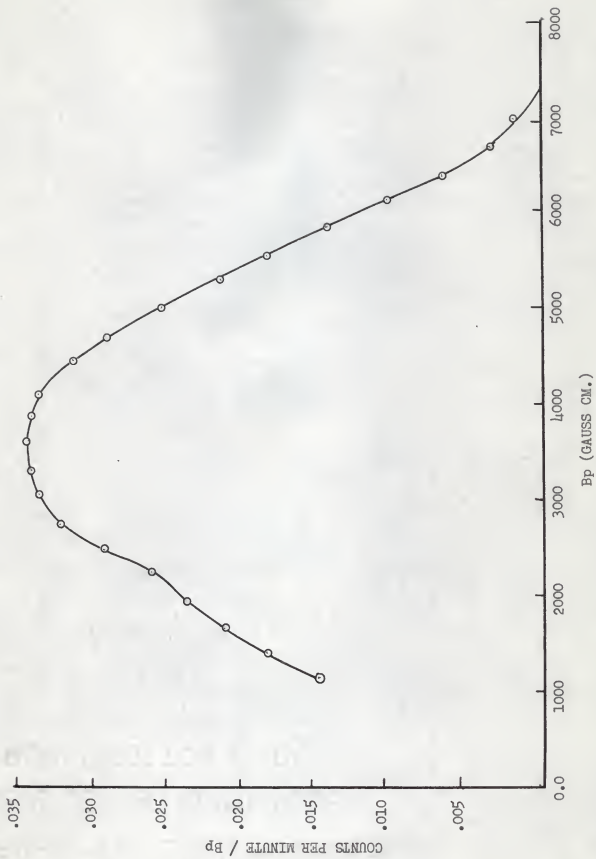
### Beta Spectrum of $P^{32}$

$N$  (counts per minute) was divided by  $E_p$  (Gauss centimeters) to obtain a normalized spectrum. Counting rates must be divided by something proportional to the magnetic field since the momentum pass band,  $\Delta(E_p)$ , is dependent on the magnetic rigidity,  $E_p$ . The former statement becomes more meaningful by considering that the resolution of a spectrometer is constant and therefore  $\frac{\Delta E_p}{E_p}$  must remain unchanged. Thus a change in  $E_p$  must be accompanied by a corresponding change in the momentum pass band.

The nature of the statistical factor is such that the beta spectrum should have a parabolic shape at the high and low energy ends. The hump shown at the low energy end of the spectrum was attributed to the presence of a contaminant isotope,  $P^{33}$ .

A residual counting rate at the high end of the spectrum gave rise to a 'tail' at energies greater than the disintegration energy of  $P^{32}$ . The internal conversion line of  $Cs^{137}$  shown in Plate III has an appreciable width at the base which was due to scattering. Thus, if the spectrum of  $P^{32}$  is thought of as being due to a continuous sum of 'lines', a slight counting rate above the end point energy would be expected. An integration over the higher energies using the shape of the line in  $Cs^{137}$  easily accounted for the tail on the  $P^{32}$  spectrum. It should be stated that the residual counting is prominent only at high energies and low counting rates.

PLATE IV

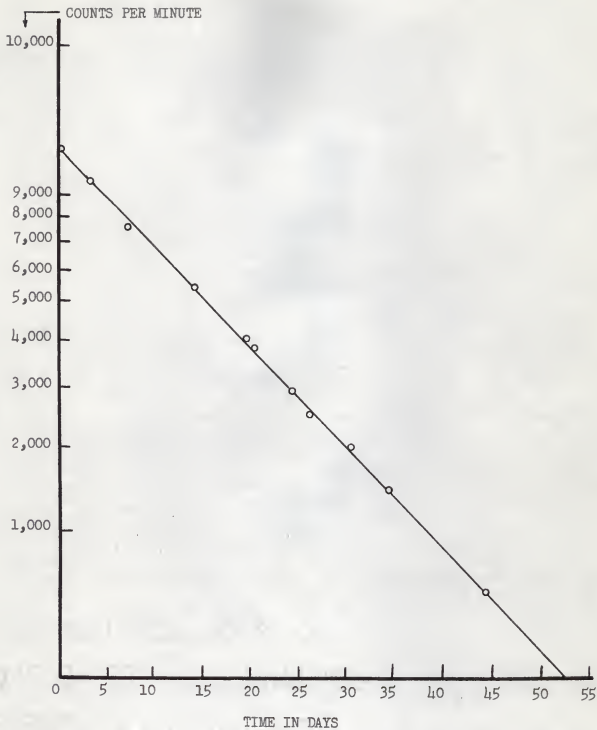


## EXPLANATION OF PLATE V

### Half-life Determination of $P^{32}$

A semi-log plot of the counting rate versus time produced a straight line whose slope gave the decay constant. To insure that only the activity of  $P^{32}$  was measured, a 6 milligram aluminum absorber was placed between the source and the counting tube. The Feather equation showed that 6 milligrams of aluminum was more than sufficient to absorb all of the  $P^{33}$  radiation. When additional absorbers were placed between the source and the counting tube it was found that a small counting rate existed even though the absorbers should have stopped all of the  $P^{32}$  radiation. A contaminate isotope could produce this effect, however, straggling seems to be the most logical explanation. Indeed if a contaminate isotope was present, it was in a very minute amount. The source was followed over forty four days and a half-life of  $14.27 \pm .05$  days was obtained.

PLATE V



hump at the low energy end of the spectrum, and second, the end point energy looked as though it was larger than the known disintegration energy.

The Fermi analysis (18) showed that the hump at the low energy end of the spectrum was produced by a contaminate beta decaying isotope (Plate VI). Further, the energy of disintegration was approximately 250 KEV. The existence of this isotope in  $P^{32}$  prepared at Oak Ridge National Laboratories has been investigated (7) and shown to be  $P^{33}$ . The amount of  $P^{33}$  present was estimated to be about 3 percent, but only meager data were taken at low energies. At low energies the electrons were unable to penetrate the mica window, therefore data in this region of the spectrum was not particularly reliable. In addition, the amount of  $P^{33}$  present depended upon the age of the radioactive stuffs; for instance, in one year the sample would be almost 97 percent  $P^{33}$  because of the difference in half-lives of the two isotopes of phosphorus. Only points well above 250 KEV were used in this investigation.

The fact that the Fermi plot gave an end point energy for the beta disintegration of  $P^{32}$  of  $1.713 \pm .005$  MEV indicated that the residual counting rate must be attributed to scattering. The effect of scattering was most noticeable when either the counting rate was low or the energy quite high. Thus the existence of a residual counting rate would not seriously hamper a small order effect investigation providing that only points sufficiently far from the end point energy were used.

If the equation for the usual Fermi plot is manipulated by dividing both sides of Equation (14) by the square of the difference between the end point energy and the energy of the electron, that is,

$$N/\{F(Z,P)p^2(E - E_0)^2\} = \text{constant} \quad (16)$$

one may detect small deviations of the Fermi plot. A plot of this nature is called a shape factor plot and should not be confused with the statistical



## EXPLANATION OF PLATE VI

### Fermi Plot

Normalized counting rate over the square of the electron momentum and the Fermi function was plotted against electron energy. The presence of two straight line segments in the Fermi plot showed that it was a complex spectrum. The change in slope at approximately 250 KEV was due to the presence of  $P^{33}$ . The intersection of the line with the electron energy axis gave the energy of disintegration of  $P^{32}$  and was found to be  $1.713 \pm .005$  MEV.

It was of particular interest to note that the "ft" value for  $P^{32}$  classifies it as second forbidden, yet the Fermi plot clearly showed it to be an allowed transition.

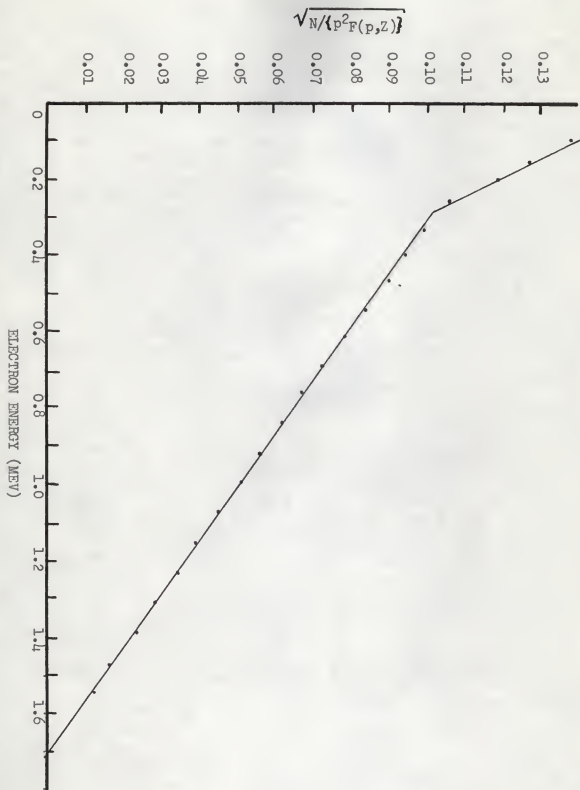


PLATE VI

shape factor. Plate VII, a statistical shape plot was obtained through such a manipulation.

The slope of Plate VI gave a direct indication of the amount by which the Fermi plot was nonlinear. Nonlinearity is exactly what would be expected if a Fierz interference were present. The plot obtained exhibits a slope of approximately 3 percent over the entire energy range investigated. It should be emphatically emphasized that the plot was extremely sensitive to the end point energy. An uncertainty in the end point energy amounting to 5 KEV could completely mask any concrete results. However, even with a 5 KEV end point uncertainty it was felt that a definite trend was established.

Had the shape factor been a straight line a Fierz interference would have been highly improbable. However, a significant slope demanded that the magnitude of the Fierz interference, which was stated before to be manifest in a constant ( $r$ ) over the energy, be obtained. It has been shown that the magnitude of the constant of the Fierz interference term could be obtained by a least-square development (12). Essentially this entailed determining the slope of the Fermi plot from a least-squares line and evaluating ( $r$ ) from the following relation:

$$r = \frac{\sum Y_{ic} / 5^{i-1} (1/W_{1i} - 2\delta)}{\sum (1/W_{1i} - 2\delta)^2} \quad (17)$$

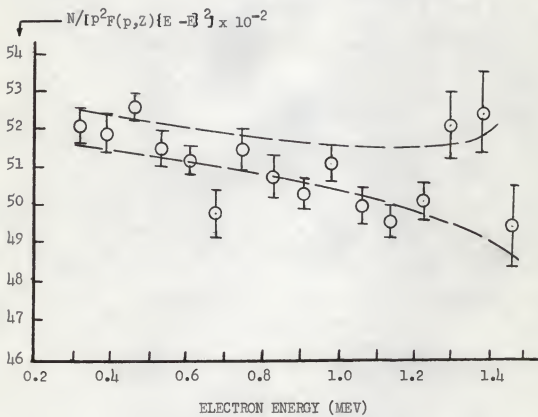
where  $Y_{ic} = N_i / [P^2 F(\epsilon, \rho) (E_0 - \epsilon)^3]$  and  $\delta = W_0 / 2W_1W_2$ .  $W_1$  and  $W_2$  are two energies between which approximately one-third of the spectrum was included. The value for ( $r$ ) obtained was  $0.07 \pm .03$ . The probable error of ( $r$ ) was determined by examining errors in the first term of Equation (17). The other terms in Equation (17) may have errors on the order of 2 or 3 percent whereas the first term could involve errors of as much as 100 percent.

## EXPLANATION OF PLATE VII

### Shape Factor Plot of Phosphorus 32

The normalized counting rate divided by the square of the electron momentum, the Fermi function, and the square of the difference between the end point energy and the electron energy was plotted against the electron energy. The error flags shown on each point were the probable errors due to counting statistics only. The dotted lines follow the local average of the points and indicate the shift of the points if the end point energy were incorrect by 5 KEV. It was difficult to obtain good statistics at extremely high energies primarily because the square of the difference between the end point energy and the electron energy was quite small and a relatively small probable error in the counting rate became large when a shape factor determination was made. This fact in itself relegates the contribution of the residual counting rate to a very slight percent of the uncertainty associated with points at the higher end of the spectrum. It was noted that the majority of the error flags were within the dotted lines. This indicated that the probable error of the end point energy of .005 MEV was a rather conservative estimate.

PLATE VII



## RESULTS AND CONCLUSIONS

The Fermi plot of Plate VI gives the following information concerning the  $\text{Na}^{32}(\text{p},\text{n})\text{P}^{32}$  reaction prepared at the Oak Ridge National Laboratories. For the beta decaying  $\text{P}^{32}$  isotope the Fermi plot should be a single straight line, however, two straight line segments were obtained. The presence of two straight line segments is due to the presence of two beta decaying isotopes. From the intersection of the line segment with the energy axis, the end point energy of  $\text{P}^{32}$  was determined to be  $1.713 \pm .005$  MEV. Also the disintegration energy of the second or contaminate isotope was found to be approximately 250 KEV and was thus attributed to the presence of  $\text{P}^{33}$ . A small percent of  $\text{P}^{33}$  was present at the onset of the investigation, however, the effect of the contaminate was eliminated since only data above the  $\text{P}^{33}$  cut off was utilized in obtaining information of  $\text{P}^{32}$ . The half-life of  $\text{P}^{32}$  was experimentally determined to be  $14.27 \pm .05$  days. The above values, within the probable errors, verify the results that have been obtained by others (17).

Most significant in this investigation is, for  $\text{P}^{32}$ , the apparent linear deviation of the Fermi plot. The deviation from a straight line is readily shown by the shape factor plot (Plate VI) to be concave upwards. The shape factor plot exhibits a slope of approximately 3 percent over the entire energy range investigated. The existence of such a slope could be attributed to the presence of a Fierz interference. The Fermi plot of  $\text{P}^{32}$  indicates that it is an allowed transition, however, the "ft" value places it in the second forbidden category where a nonlinear Fermi plot is characteristic. If the problem of classification of forbiddenness is resolved and shown to be second forbidden then this investigation makes no contribution to the problem of the exact form of beta decay. If, on the other hand, the  $\text{P}^{32}$  transition is later shown



to be allowed then the STP combination proposed by Mahmoud and Konopinski is quite impossible. Further, an exact form representing beta decay must include both the tensor and axial-vector interaction energy terms.

If the transition of  $P^{32}$  is allowed, this experiment becomes quite important and refinements would be desirable. Therefore the following suggestions are set forth as a means whereby the probable error associated with the shape factor plot may be reduced.

As in all nuclear experiments high counting rates are very desirable, here again this becomes extremely important. A higher counting rate and more uniform source may be obtained by employing vacuum evaporation techniques (19). The backing described in this paper should prove to be adequate to minimize back scattering. The  $P^{32}$  source should be obtained from the Chalk River pile because  $P^{32}$  produced there has been shown to be free of  $P^{33}$  (7). A source free of  $P^{33}$  would allow the low energy region of the  $P^{32}$  spectrum to be utilized. It is quite important that the low energy region of the  $P^{32}$  spectrum be exploited, primarily because here the difference between the end point energy and the beta particle energy is largest. It is this energy difference which is used as a divisor in computing the shape factor plot. Hence the probable error of the shape factor plot is smallest at the low energy region.

## ACKNOWLEDGMENT

Sincere thanks and appreciation is due Dr. Robert Kats for his timely advice and expert help in the preparation of this paper. Thanks is also extended to Dr. Moser of the Department of Chemistry for making the radioactive phosphorus available. In addition, the author would like to take this opportunity to thank each member of the Physics Staff for their interest in this research.

## LITERATURE CITED

- (1) Agnew, Harold M.  
The beta-spectra of Cs<sup>137</sup>, Y<sup>91</sup>, Pa<sup>214</sup>, Ru<sup>106</sup>, Sm<sup>152</sup>, P<sup>32</sup>, and Tm<sup>170</sup>.  
Phys. Rev. 83:655-660. 1950.
- (2) Blatt, John M. and Victor F. Weisskopf.  
Theoretical nuclear physics. New York: Wiley, 705-718;  
677-678. 1952.
- (3) Brossi, Bruno.  
Ionisation chambers and counters. New York: McGraw Hill,  
115-117. 1949.
- (4) Davidson, J. P. and D. C. Peaslee.  
Cross terms in allowed shape spectra. Phys. Rev. 91:1232-1233.  
1953.
- (5) Fermi, E.  
Versuch einer theorie der beta strahlen. Zeits. F. Physik.  
88:161-177. 1934.
- (6) Fierz, Markus Von.  
Zur fermischen theorie des  $\beta$ -zerfalls. Zeits. F. Physik.  
104:553-565. 1937.
- (7) Jensen, Erling N., Nichols, R. T., Clement, J., and A. Pohn.  
The beta-spectra of P<sup>32</sup> and P<sup>33</sup>. Phys. Rev. 85:112-119. 1952.
- (8) Katz, Robert and Milford R. Lee.  
Variable field beta-ray spectrometer-spectrograph. Rev. Sci. Inst.  
25:58-62. 1954.
- (9) Mahmud, H. M. and E. J. Konopinski.  
The evidence of the once-forbidden spectra for the law of decay.  
Phys. Rev. 88:1266-1275. 1952.
- (10) Orear, J., Rosenfeld, A. H., and R. A. Schluter.  
Nuclear physics: a course given by Enrico Fermi at the University  
of Chicago. Chicago: The University of Chicago Press, 1950. 76 p.
- (11) Porter, F. T., Wagner, F. Jr., and M. S. Freedman.  
Evidence for small deviations from the allowed shape in the  
comparison of the beta spectra of Na<sup>24</sup> and P<sup>32</sup>. Phys. Rev.  
107:135-138. 1957.
- (12) Pohn, A. V., Waddell, R. C., and E. N. Jensen.  
Small-order effects in beta spectra. Phys. Rev.  
101:1315-1321. 1956

- (13) Shiff, Leonard I.  
Quantum mechanics. New York: McGraw Hill, 1955. 197 p.
- (14) Sheline, Raymond K., Holtzman, Richard B., and Chang-Yun Fan.  
The nuclide  $P^{33}$  and the  $P^{32}$  spectrum. Phys. Rev. 83:919-922. 1951.
- (15) Sherwin, C. W.  
Experiments on the emission of neutrinos from  $P^{32}$ .  
Phys. Rev. 82:52-57. 1951.
- (16) Siegbahn, Kai.  
Beta- and gamma-ray spectroscopy. New York: Interscience  
Publishers, 276-277; 227; 280. 1955.
- (17) Strominger, D., Hollander, J. M., and G. T. Seaborg.  
Table of isotopes. Revs. Modern Phys. 30:614. 1958.
- (18) Tables for the analysis of beta spectra.  
Mat'l. Bur. Stand. Applied Mathematics Series 13. 1952.
- (19) Warshaw, S. D., Chen, J. J. L., and G. L. Appleton.  
The beta spectrum of  $P^{32}$ . Phys. Rev. 80:288. 1950.
- (20) Ether-resin wax; obtained through the courtesy of Dupont Laboratories.

THE BETA SPECTRUM STUDY OF  
RADIOACTIVE PHOSPHORUS

by

RANDALL EDWARD MURPHY

B. S., Washburn Municipal University, 1956

---

AN ABSTRACT OF A THESIS

submitted in partial fulfillment of the

requirements for the degree

MASTER OF SCIENCE

Department of Physics

KANSAS STATE UNIVERSITY  
OF AGRICULTURE AND APPLIED SCIENCE

1959

The type of interaction that takes place in a beta decaying nucleus is known to be a combination of five forms. Accumulated experimental evidence has led Mahmoud and Konopinski to propose a Scalar-Tensor-Pseudo-scalar combination as the exact form of the interaction in beta decay. This proposal was investigated experimentally through the use of phosphorus 32.

Samples of  $P^{32}$  obtained from the Oak Ridge National Laboratories contained a slight trace of phosphorus 33. The half-life of  $P^{32}$  was experimentally determined to be  $14.27 \pm .05$  days and this value was used in the Fermi analysis of the  $P^{32}$  spectrum. The disintegration energy of  $P^{32}$  obtained was  $1.713 \pm .005$  MEV. These results were in good agreement with the values obtained by others.

The shape factor plot of  $P^{32}$  exhibited a slope of three percent over the entire energy range investigated. A definite slope showed that the Fermi plot of  $P^{32}$  was concave upwards and could be caused by a Fiers interference. The possibility of an STP combination seems rather remote in view of the deviation from a straight line. In general the distinction between an allowed or a second forbidden spectrum is made on the basis of the shape of the Fermi plot and the "ft" value. These two criteria do not yield the same result for  $P^{32}$ . The Fermi plot indicates an allowed spectrum while the "ft" value implies a second forbidden spectrum. This discrepancy is not resolved in the present investigation. If later evidence shows the spectrum to be second forbidden these data make no contribution to the question of the nature of the beta decay interaction. If the spectrum is later shown to be allowed then the present results imply that the STP combination proposed by Mahmoud and Konopinski is not possible.